Cell Reports, Volume *18*

Supplemental Information

Coupling between Protein Stability and Catalytic Activity Determines Pathogenicity of G6PD Variants

Anna D. Cunningham, Alexandre Colavin, Kerwyn Casey Huang, and Daria Mochly-Rosen

Supplemental Figures and Tables

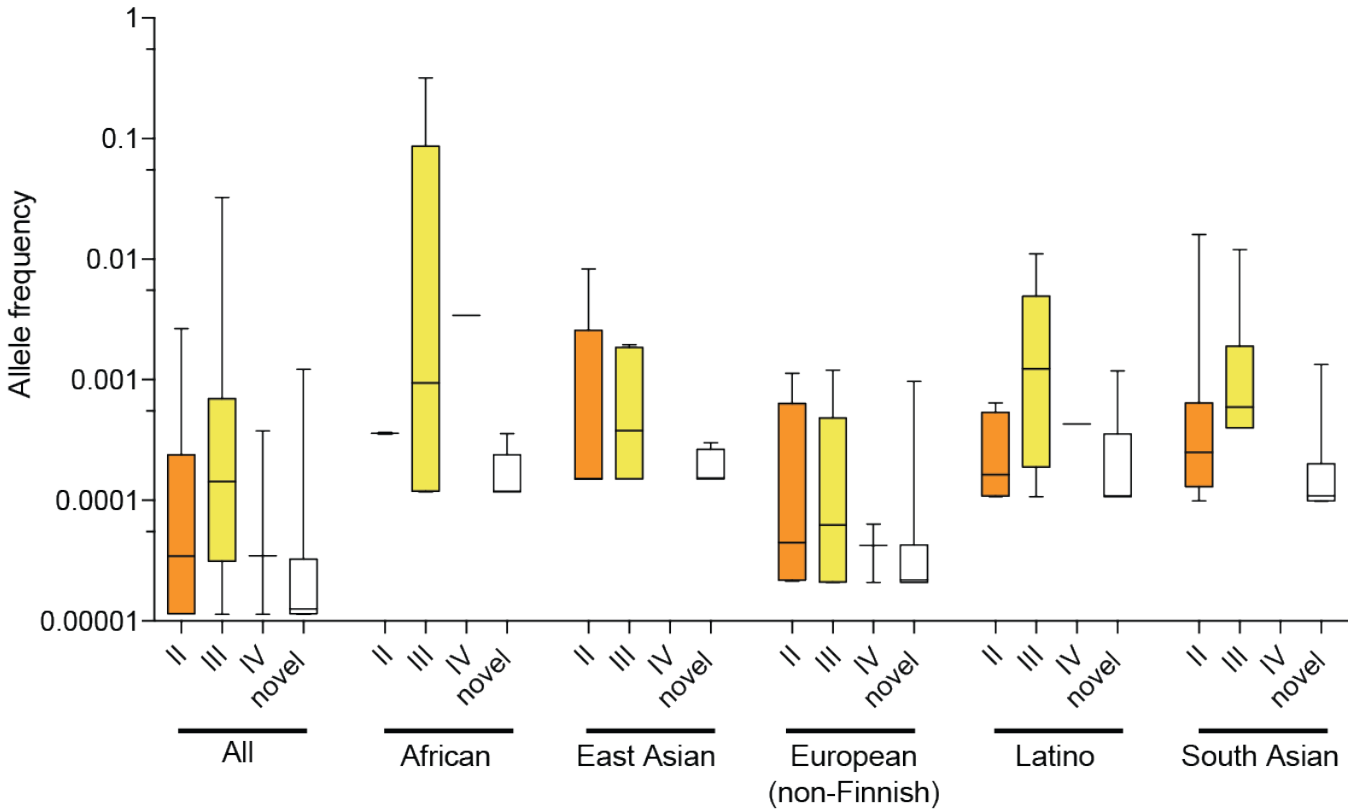

Figure S1: Allele frequencies of previously known and uncharacterized G6PD variants in the ExAC database. Related to Figure 2. Allele frequencies of G6PD variants in each population (Tables S1, S2) are plotted, separated by class. The Finnish population is omitted due to the low number of variants observed in this population.

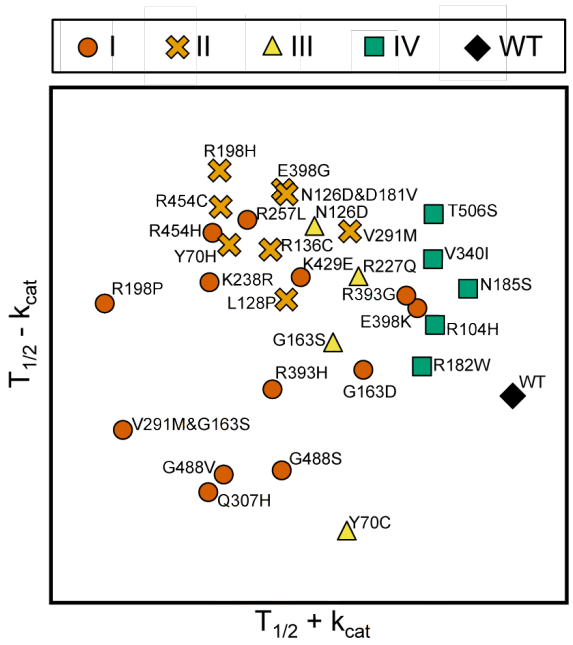

Figure S2: Labeled PCA-like plot. Related to Figure 4. PCA-like plot of variants from this study and other studies, labeled corresponding to each variant (data are the same as in Fig. 4A).

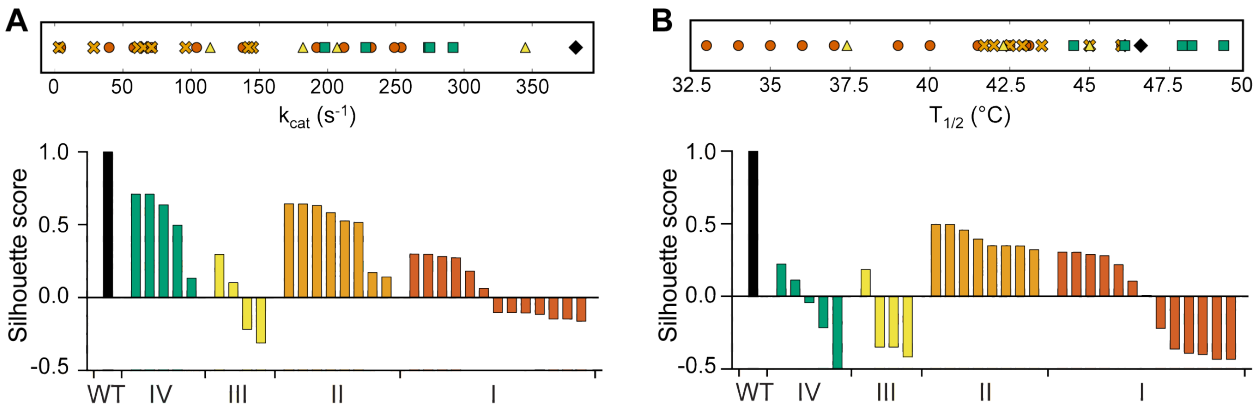

Figure S3: Separation of G6PD variants along individual biochemical parameters. Related to Figure 4.

A) k_{cat} values of variants from this study and other studies (top) and silhouette scores resulting from clustering (bottom).

B) $T_{1/2}$ values of variants from this study and other studies (top) and silhouette scores resulting from clustering (bottom).

Table S1: Uncharacterized G6PD variants in the ExAC database. Related to Figure 2. Variants characterized in this study are highlighted in yellow.

See separate Excel file.

Table S2: Previously identified G6PD variants in the ExAC database. Related to Figure 2.

See separate Excel file.

Table S3: Biochemical parameters of G6PD variants in this study. *h* is the fitted Hill coefficient. Related to Figure 3A.

Variant	Class	SIFT	PolyPhen2	K_M $NADP^+$ (μM)	*h* $NADP^+$	K_M G6P (μM)	*h* G6P	k_{cat} (s^{-1})	$T_{1/2}$ (°C)
WT	--	--	--	16.3 ± 0.6	2.3	106 ± 4	1.6	382 ± 8	46.6 ± 0.1
Y70H	II	0	0.999	34 ± 4	2.2	143 ± 18	1	61 ± 5	41.7 ± 0.2
Y70C	III	0	1	21 ± 2	2.5	92 ± 5	3	345 ± 12	37.4 ± 0.3
R198P	I	0	1	38 ± 2	1.5	26 ± 4	1	4.4 ± 0.2	36.0 ± 0.2
R198H	II	0	1	48 ± 3	1.5	81 ± 19	0.7	3.2 ± 0.2	43.5 ± 0.2
Q307H	I	0	1	14.7 ± 0.6	2.3	83 ± 3	2.3	212 ± 5	34.0 ± 0.2
Q307P	III	0	1	--	--	--	--	--	--
E398K	I	0	1	16.3 ± 0.3	2.7	78 ± 3	2.8	249 ± 7	46.0 ± 0.2
E398G	II	0	1	11 ± 1	1.7	47 ± 5	1.6	65 ± 4	45.0 ± 0.1
R104H	--	0.62	0.106	16.1 ± 0.5	3.9	98 ± 4	1.5	274 ± 6	46.1 ± 0.1
R182W	--	0	0.437	20 ± 1	2	145 ± 10	1	292 ± 9	44.5 ± 0.1
N185S	--	0.91	0	17 ± 1	3.3	94 ± 7	1	275 ± 10	48.2 ± 0.1
V340I	--	0.66	0.047	20 ± 1	2.7	119 ± 12	1	228 ± 9	47.9 ± 0.1
T506S	--	0.74	0.008	18.9 ± 0.9	2.8	107 ± 12	1	198 ± 8	49.2 ± 0.1

Table S4: Biochemical parameters of G6PD variants from other studies that are used in this study. Related to Figure 4.

Variant	Class	K_M $NADP^+$ (µM)	K_M G6P (µM)	k_{cat} (s^{-1})	$T_{1/2}$ (°C)	Reference
K429E	I	6.4	39.9	138	43.1	(Gómez-Manzo et al., 2014)
R136C	II	3.6	21.5	96	42.9	(Gómez-Manzo et al., 2014)
R227Q	III	9.1	24.9	182	45	(Gómez-Manzo et al., 2014)
R393H	I	31.2	90.6	119	44.3	(Gómez-Manzo et al., 2014)
K238R	I	6.96	24.77	71	40	(Gómez-Manzo et al., 2015)
N126D & D181V	II	9.06	15.35	71	45	(Gómez-Manzo et al., 2015)
N126D	III	12.97	56.44	114	45	(Gómez-Manzo et al., 2015)
R393G	I	9.31	67.1	232	46	(Wang and Engel, 2009)
R393H	I	16.5	190	192	39	(Wang and Engel, 2009)
G488V	I	10.7	53.8	212	35	(Wang and Engel, 2009)
G488S	I	11.8	49.1	254	37	(Wang and Engel, 2009)
R454C	II	2.76	9.53	28.6	42.5	(Wang et al., 2005)
R454H	I	2.38	9.71	39.9	41.5	(Wang et al., 2005)
G163D	I	4.8	44.4	249	42.5	(Huang et al., 2008)
G163S	III	6.46	50.7	207	42.3	(Huang et al., 2008)
R257L	I	24	111	58	43	(Gómez-Manzo et al., 2016)
V291M	II	17	42	145	46	(Gómez-Manzo et al., 2016)
L128P	II	18	34	142	42	(Gómez-Manzo et al., 2016)
V291M	II	34.1	56.3	116	38	(Boonyuen et al., 2016)
V291M & G163S	I	55.9	54.3	104	33	(Boonyuen et al., 2016)

Supplemental Experimental Procedures

Cloning and mutagenesis of plasmid constructs

Wild-type G6PD cDNA was inserted into the pET-28a vector with a 6xHis tag linked by a thrombin cleavage site, using NdeI and SalI restriction sites. Mutagenesis to obtain G6PD variants was performed by the GenScript USA Inc (Piscataway, NJ) mutagenesis service.

Enzyme purification

Proteins were expressed in *E. coli* C43(DE3). Bacteria were grown at 37 °C until OD_{600} = 0.4-0.5, then expression was induced with 0.5 M IPTG for 4 h. Bacterial pellets were suspended in lysis buffer (50 mM Tris, 300 mM NaCl, 5% glycerol, 0.4 mM PMSF, 1 mg/mL lysozyme, 0.1% Triton X-100, protease inhibitor cocktail (Sigma, St Louis, MO), pH 7.8) and lysed by sonication. Lysate was clarified by spinning at 30,000*g* for 30 min, and supernatant was loaded onto 1 mL TALON Superflow beads (GE Healthcare, Pittsburgh, PA) for 1 h at 4 °C with rocking. Beads were washed with 30 mL wash buffer (50 mM Tris, 300 mM NaCl, 20 mM imidazole, pH 7.8) and resuspended in 2 mL PBS. 50 Units thrombin (R-BioPharm, Darmstadt, Germany) were added and beads were incubated overnight at 4 °C with rocking. The eluate was then purified on Superdex 75 gel filtration column (GE Healthcare) in buffer: 50 mM Tris, 150 mM NaCl, 0.5 mM EDTA, pH 7.4. Fractions containing G6PD were concentrated using a Vivaspin-6 30 kD MWCO spin column (GE Healthcare) and stored in 40% glycerol, 1 mM EDTA, 1 mM DTT at -80 °C. Protein concentration was measured using the Protein Assay Dye Reagent (Bio-Rad, Hercules, CA).

Enzyme activity and stability measurements

Enzyme activity was determined following the WHO protocol (Organization, 1989), using 0.1–0.5 µg/mL G6PD and 100 mM Tris, 0.5 mM EDTA, 10 mM $MgCl_2$, pH 8.0, and varying concentrations of G6P (Sigma) and $NADP^+$ (98% pure, Sigma).

For K_M and k_{cat} measurements, G6P concentration was kept constant at 500 µM while $NADP^+$ was varied from 1 to 200 µM, or $NADP^+$ concentration was kept constant at 200 µM while G6P was varied from 5 µM to 1 mM. Production of NADPH was determined by measuring fluorescence on a Flexstation II microplate reader (Molecular Devices Corporation, Sunnyvale, CA) using the NADPH-diaphorase-resazurin coupled reaction (Zhu et al., 2009). Relative Fluorescence Unit (RFU) values were then converted to NADPH concentration using a standard NADPH curve (NADPH 97% pure, Sigma).

For $T_{1/2}$ measurements, 2 µg/mL enzyme was incubated with 5 µM $NADP^+$ for 20 min at temperatures ranging from 25 °C to 65 °C, then placed on ice for 5 min. Activity was then assayed by measuring NADPH via absorbance at 340 nm on a Bio-Rad Benchmark Plus microplate reader (Bio-Rad Laboratories, Inc., Hercules, CA).

Data were analyzed using GraphPad Prism v. 6.0a (GraphPad Software, La Jolla, California USA). To obtain kinetic parameters, the data were fitted using the preset nonlinear regression equations *Michaelis-Menten* and *Allosteric sigmoidal*. The best fit was selected using the *Compare* feature, and the following parameters were reported: k_{cat}, K_M, and *h* (Hill coefficient, equal to 1 when *Michaelis-Menten* was the best fit). For $T_{1/2}$, the data were fit using the *Boltzmann sigmoidal* equation and the *Top* and *Bottom* values were set to 0 and 100, respectively. All values are reported as mean ± standard error.

Interestingly, we found that WT G6PD exhibited allosteric sigmoidal kinetics rather than Michaelis-Menten kinetics, which could be explained by the presence of multiple independent active sites in dimeric or tetrameric G6PD (Sweeny and Fisher, 1968). Furthermore, G6PD contains two binding sites for $NADP^+$ per monomer, so allosteric sigmoidal kinetics may be explained by binding cooperativity between these two sites.

Supplemental References

Organization, W.H. (1989). Glucose-6-phosphate dehydrogenase deficiency. WHO Working Group. Bulletin of the World Health Organization *67*, 601-611.

Sweeny, J.R., and Fisher, J.R. (1968). Alternative to allosterism and cooperativity in the interpretation of enzyme kinetic data. Biochemistry *7*, 561-565.

Zhu, A., Romero, R., and Petty, H.R. (2009). An enzymatic fluorimetric assay for glucose-6-phosphate: application in an in vitro Warburg-like effect. Analytical biochemistry *388*, 97-101.